RESEARCH NOTES

RESISTANCE OF IMPINGING STREAM CONTACTOR TO SOLID-AIR SUSPENSION FLOW*

Wu Gaoan(吴高安)**and Wu Yuan(伍　沅)***

Department of Chemical Engineering, Zhejiang University of Technology, Hangzhou 310014, China

1 INTRODUCTION

As mentioned in our previous paper[1] impinging stream contactor (ISC) is an innovative device for phase contact operations and has proved itself capable to enhance transfer processes in heterogeneous systems effectively, and thus is of potential application in many chemical engineering processes, such as drying of solid particles, solid-solid, liquid-liquid and gas-gas mixing, absorption and desorption of gases into or from liquids with or without chemical reactions, combustion of liquid fuel or coal, etc.[2]. One of the problems at great concern, and perhaps most[3] challenging, is the power requirement for ISC operation. Tamir et al.[4-7] investigated total pressure drops across ISCs of various designs and dimensions for particles-gas systems. However, their measured data were so very diversified, from 20 to 3725 Pa, failing to throw a light on the generalization of the power requirement, and failed to cope with predicted values calculated from a method proposed by the same authors[2]. It is noted that, likely, both the facts that certain complex flow configurations are tested, which are inessential for ISC application, e.g., tangential flow, multi-pair of impinging streams (IS), and multi-stage ISCs etc., and that small dimensions of ISC used in most of their experiments introduce additional resistance to suspension flows.

In the present paper, the resistance of an ISC is studied theoretically and experimentally in terms of total drop in pressure (DP) across the ISC and its constituents, with emphasis on those resulted from acceleration of particles and impingement between streams, both which are essential in ISC operations.

2 THEORETICAL CONSIDERATION

The resistance of an ISC to streams is resulted essentially from three factors: (1) Friction due to the twophase flows through the accelerating pipes, (2)Impingement

between the two streams, and (3) Design of the ISC, *e. g.*, contraction of the cross-section area at the air outlet and/or other structural parts.

2.1 Flow through accelerating pipes

Several factors, such as skin friction of air flow in the pipes, acceleration of particles by air, and collision of particles on the wall and between particles *etc.*, result in DP along the pipes. For convenience, it may be considered to consist of two constituents caused by air and particles, $-\Delta p_{ac,a}$ and $-\Delta p_{ac,p}$, respectively.

2.1.1 *Resistance due to air flow*

The DP due to friction of gas flow in the of accelerating pipes, $-\Delta p_{ac,a}$, can be predicted generally by

$$-\Delta p_{ac,a} = \lambda_a \frac{L_{ac}}{d} \frac{\rho_a u_a^2}{2} \tag{1}$$

where the friction coefficient, λ_a, is a function of both relative roughness ε/d and Reynolds number Re_a, and the well-known graph of λ_a vs Re via ε/d can be found in Ref.[8]. The air velocity in Eq.(1), u_a, is theoretically affected by both the local pressure and the existence of particle under isothermal conditions, while, in practice, it can be taken as constant for that the DP across accelerating pipe is very small in comparison with operating pressure and that suspensions processed are usually dilute, say, $m_p/m_a = 0.5 - 2.0$, yielding very small volume fraction of particles in suspension ($\leqslant 0.5\%$).

2.1.2 *Pressure drop due to particles movement*

The overall energy balance of the system, air plus particles, round an accelerating pipe can be written as

$$\text{(input)} \quad 0 \quad + \frac{1}{2} m_a u_a^2 + p_1 \frac{m_a}{\rho_a} = \frac{1}{2} m_{po} u_{po}^2 + \frac{1}{2} m_a u_a^2 + p_2 \frac{m_2}{\rho_a} \quad \text{(output)} \tag{2}$$
$$\text{particles} \qquad \text{air flow} \qquad \text{particles} \qquad \text{air flow}$$

Rearranging Eq.(2) yields

$$-\Delta p_{ac,pl} = p_1 - p_2 = \frac{1}{2} \rho_a \frac{m_p}{m_a} u_{po}^2 \tag{3}$$

Eq.(3) defines the minimum DP resulted from particle flow through the accelerating pipe, in which u_{po} is the mean velocity of particles at the outlet of the accelerating pipe, depending on air velocity u_a, length of the pipe L_{ac}, density ratio ρ_p/ρ_a, and mean diameter of particles d_p, and can be determined by the motion equations below

$$\frac{du_p}{dt} = 0.75 C_f [\frac{\rho_a}{\rho_p d_p}] (u_a - u_p)^2 \tag{4}$$

$$u_p \frac{du_p}{dl} = 0.75 C_f [\frac{\rho_a}{\rho_p d_p}] (u_a - u_p)^2 \tag{5}$$

with the initial conditions

$$u_p = 0 \text{ and } l = 0, \text{ at } t = 0 \tag{6}$$

where the drag force coefficient, C_f, depends on flow pattern and the well-known relationships between C_f and Re_p for the Stokes, transition and turbulent regions can be found, e.g., in Ref. [8], with Re_p being defined as

$$Re_p = \frac{d_p \rho_a}{\mu_a} |u_a - u_p| \tag{7}$$

On the other hand, collisions of particles on the inside wall of the pipes and between particles also causes a DP, $-\Delta p_{ac,p2}$. Some authors consider it as a proportion of that resulted by pure air flow[9], while it would be more reasonable and convenient to have it related to $-\Delta p_{ac,p1}$, because both the two kinds of collisions are affected directly by the same parameters as $-\Delta p_{ac,p1}$. In this way, we have

$$-\Delta p_{ac,p2} = a(-\Delta p_{ac,p1}) = a(1/2)\rho_a(m_p/m_a)u_{po}^2 \tag{8}$$

where a is a proportional factor. Define the combined local resistance coefficient

$$\zeta_{ac,p} = 1 + a \tag{9}$$

then the DP caused by both acceleration and collision of particles can be expressed to be

$$-\Delta p_{ac,p} = -(\Delta p_{ac,p1} + \Delta p_{ac,p2}) = \zeta_{ac,p}(1/2)\rho_a(m_p/m_a)u_{po}^2 \tag{10}$$

Thus, the summation DP throughout the accelerating pipes is

$$-\Delta p_{ac} = -(\Delta p_{ac,a} + \Delta p_{ac,p}) \tag{11}$$

2.2 Impingement between streams

It is found in the experiments that the DP due to impingement of streams is independent of particle existence. To estimate it by an energy or momentum balance is difficult, since the impingement zone has no definite boundary so that the radial velocity of air leaving this zone cannot be determined. It may be considered from observation that the impinging plane serves like a number of $90°$-turning tubes without definite diameter in the sense of producing a resistance to air flow. Thus, an equivalent "local resistance coefficient", ζ_{im}, may be used to express

$$-\Delta p_{im} = \zeta_{im}\rho_a u_a^2/2 \tag{12}$$

2.3 Resistance resulted from design of ISC

Some design factors, such as changes in cross-section area and direction of flow etc., lead also to DPs, while they vary from ISC to ISC. For generalization, all design factors may be expressed with a combined local resistance coefficient, ζ_{ds}, related to the air velocity in the accelerating pipe, u_a, for convenience, i.e.,

$$-\Delta p_{ds} = \zeta_{ds}\rho_a u_a^2/2 \tag{13}$$

and such a coefficient can be determined according to the specific ISC design with common method, e.g., as given in Ref.[8]. For the ISC studied here (see Fig. 1), DPs may be caused by the two factors: (1) $180°$-turning of flow resulted from the blind, and (2) the sudden contraction of the cross section area for air flow at its

outlet. The former is negligible for the local air velocity is very small (<0.05 m $\cdot$ s^{-1}), while the latter is comparable with that caused by impingement and can be expressed generally by

$$-\Delta p_{ao}=\zeta_{ao}\rho_a u_{ao}^2/2 \tag{14}$$

where ζ_{ao} can be taken as unity from Ref. [8], while u_{ao} is the air velocity in the outlet tube and can be determined by the continuity equation as

$$u_{ao}=(d/d_o)^2 u_a \tag{15}$$

Thus, Eq.(13) is specified for the ISC under consideration, as

$$-\Delta p_{ds}=(d/d_o)^4 \rho_a u_a^2/2 \tag{16}$$

2.4 Total pressure drop across an ISC
Now, the total DP across an ISC can be expressed as

$$-\Delta p_T = -(\Delta p_{ac,a}+\Delta p_{ac,p}+\Delta p_{im}+\Delta p_{ds}) \tag{17}$$

where $-\Delta p_{ac,a}$, $-\Delta p_{ac,p}$, $-\Delta p_{im}$ and $-\Delta p_{ds}$ are represented by Eqs(1), (10), (12) and (13), respectively, in which λ_a and ζ_{ds} can be predicted with the common methods according to the design of the ISC used, while $\zeta_{ac,p}$ and ζ_{im} remain to be determined.

3 EXPERIMENTAL EQUIPMENT AND PROCEDURE
The ISC used in the present study is of two coaxial horizontal jets, as shown in Fig.1, with its main dimensions. Two air streams flow at the same rate through
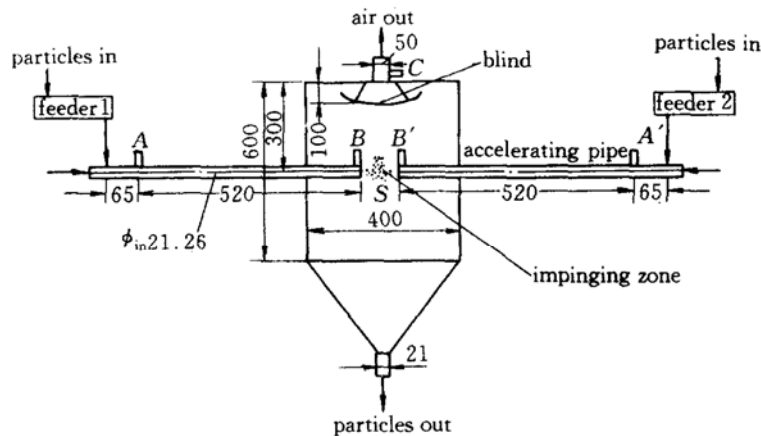

Figure 1 Impinging stream contactor with two coaxial horizontal jets (unit: mm)

the accelerating pipes to speed up the particles fed-in by Feeders 1 and 2, respectively, to a certain fraction of the air velocity, and then oppositely inject at the same velocity into the impingement zone. Both the pipes are of the same diameter and length, and the impinging distance between Points B and B' in Fig. 1 is changeable. The horizontal cross section of the upper plexiglass chamber is a

square of 0.4×0.4m, and the bottom is tapered sharply. The accelerating pipes are zinc-plated steel tubing with a relative roughness of $\varepsilon/d = 0.0047$. Both the screw feeders 1 and 2 are driven by motors with precisely manipulated rotating speeds so that they supply the ISC with particles at stable flow rates.

The solid materials tested are millets and rape seeds with the properties listed in Table 1. All the experiments are carried out at room temperature, and the ranges of operating conditions studied are: air velocity in accelerating pipes $u_a = 9.48 - 17.36$ m $\cdot$s^{-1}, mass flow ratio $m_p/m_a = 0.556 - 1.0$, and non-dimensional impinging distance $S/d = 3.0 - 6.7$.

Table 1   Properties of the materials used in the experiments

Property	ρ_p, kg $\cdot$ m^{-3}	ρ_b, kg $\cdot$ m^{-3}	$d_p \times 10^3$, m
millets	1101	661.5	1.6872
rape seeds	1172	696.5	1.6304

DPs are measured between the Points A and C, A' and C, A and B, and A' and B', denoted by $-\Delta p_{AC}$, $-\Delta p_{A'C}$, $-\Delta p_{AB}$, and $-\Delta p_{A'B'}$ respectively, with inclined U-shape tubes filled with coloured kerosene. The average of $-\Delta p_{AB}$ and $-\Delta p_{A'B'}$ is taken as the DP through the accelerating pipes, $-\Delta p_{ac}$, and that of $-\Delta p_{AC}$ and $-\Delta p_{A'C}$ as the overall DP of the ISC, $-\Delta p_T$. Consequently, there should be

$$-(\Delta p_{im} + \Delta p_{ds}) = -\Delta p_T - (-\Delta p_{ac}) \qquad (18)$$

4   RESULTS AND DISCUSSION
4.1   Essential characteristics of pressure drop distribution
Table 2 gives two sets of typical data measured for DPs, as instances, at various mass flow ratio. All the other results exhibit the same nature of DP distribution as given in Table 2, too, which is characterized by the following: (1) The majority of the resistance ($\geqslant 80\%$) to the streams, no matter pure air or particles-in-air suspensions, occurs in the accelerating pipes, as $-\Delta p_{ac}$, (2) The presence of particles in the streams does not exhibit any substantial influence on both the DPs resulted from impingement and caused by design factors of the ISC, $-\Delta p_{im}$ and $-\Delta p_{ds}$, while (3) The presence of particles increases the DP in accelerating pipes significantly.

A very important observation obtained from the characteristics (1) and (3) is that most of the power needed for an ISC operation is being consumed for the acceleration of the particles.
4.2   Resistance of accelerating pipe to pure air flow
Fig.2 shows the effects of air velocity and non-dimensional impinging distance on $-\Delta p_{ac,a}$, As can be seen, $-\Delta p_{ac,a}$ is essentially constant for $S/d \geqslant 4.0$, while in the range < 4.0, S/d exhibits a small influence, i. e., $-\Delta p_{ac,a}$ increases slightly with decreasing S/d. Furthermore, all the data for $-\Delta p_{im}$ show the same tendency as well. These results are essentially consistent with the data obtained by Elperin[10] for the axial profile of static pressure in an ISC. It is also found that, as S/d

decreases in the range <4.0, fluctuation of pressure at the outlets of the accelerating pipes increases and the stability of impingement zone becomes poorer. Therefore the value of 4.0 for S/d may be taken as the lower limit for application of ISC for gas-solid systems. Thus, it can be considered that $-\Delta p_{ac,a}$ is independent of S/d in the range of practical interest.

Table 2 Data for pressure drop distribution ($u_a = 14.22$m $\cdot$ s^{-1}, $S/d=4.0$)

m_p/m_a	Millets					Rape seeds				
	$-\Delta p_T$, Pa	$-(\Delta p_{im}+\Delta p_{ds})$,Pa	$a^{①}$,%	$-\Delta p_{ac}$,Pa	$b^{②}$,%	$-\Delta p_T$,Pa	$-(\Delta p_{im}+\Delta p_{ds})$,Pa	$a^{①}$,%	$-\Delta p_{ac}$,Pa	$b^{②}$,%
0.0	87.36	15.65	17.9	71.71	82.1	83.38	12.32	14.8	71.06	85.2
0.556	133.64	13.69	10.2	119.95	89.8	142.70	15.06	10.5	127.64	89.5
0.588	140.88	16.82	11.9	124.06	88.1	144.33	15.58	10.8	128.75	89.2
0.625	139.96	15.45	11.0	124.51	89.0	144.00	14.60	10.1	129.40	89.9
0.667	140.48	14.34	10.2	126.14	89.8	147.01	14.80	10.1	132.21	89.9
0.714	144.07	14.34	10.0	129.73	90.0	150.53	15.06	10.0	135.47	90.0
0.769	149.29	14.67	9.8	134.62	90.2	153.66	14.67	9.5	138.99	90.5
0.833	150.73	13.76	9.1	136.97	90.9	163.36	16.75	10.2	146.61	89.8
0.909	152.22	13.69	9.0	138.53	91.0	167.34	15.12	9.0	152.22	91.0
1.0	162.32	20.01	12.3	142.31	87.7					

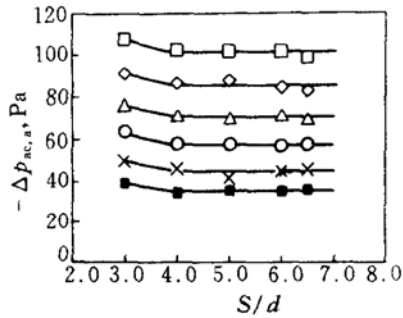① $a = \dfrac{-(\Delta p_{im}+\Delta p_{ds})}{\Delta p_T} \times 100$ ② $b = \dfrac{-\Delta p_{ac}}{\Delta p_T} \times 100$

Figure 2 Influences of air velocity and nondimensional
impinging distance on $-\Delta p_{ac,a}$

u_a,m$\cdot$s^{-1}: ■ 9.48; × 11.06; ○ 12.64;
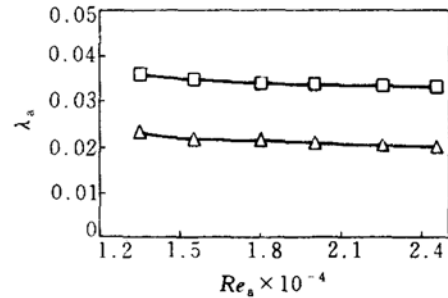△ 14.22; ◇ 15.80; □ 17.30

Figure 3 Friction coefficient of air flow
($\varepsilon/d = 0.0047$)

□ from Ref.[8]; △ measured

The air velocity in the accelerating pipes, u_a, has significant effect on $-\Delta p_{ac,a}$, as can be seen in Fig.2 as well as predicted with Eq.(1). Calculations are made by Eq.(1) using the experimental data for the values of friction coefficient, and the results are given in Fig.3, in which data from the graph in Ref. [8] for the same parameter are also shown for comparison. The influences of Re_a on λ_a experimentally measured or taken from Ref. [8] exhibit the same tendency, while the measured values for λ_a are smaller than those obtained from Ref. [8] by about 1.5 times. The reason for this is not clear yet. A linearized regression of the measured data leads to

$$\lambda_a = 0.02131 Re_a^{0.000118} \qquad (19)$$

Therefore, λ_a can actually be considered to be independent of Re_a in the range of interest, and a value of 0.0214 may be taken for it. In addition, as a first order approximation, the value for λ_a may be taken from the graph of λ_a vs Re_a given in Ref. [8] from the dimensions of accelerating pipes in an ISC without significant error, as the related constituent occupies only a very small fraction in the total DP.

4.3 Pressure drops caused by acceleration and collisions of particles

The values for $-\Delta p_{ac,p}$ can be calculated with Eq.(11) from the data for $-\Delta p_{ac}$. Significant effects of both particle velocity at the outlet of the accelerating pipe, u_{po}, and mass flow ratio, m_p/m_a, on $-\Delta p_{ac,p}$ are observed, as shown partly in Fig.4. The "local" resistance coefficient, $\zeta_{ac,p}$, is also calculated with Eq.(10) from the data obtained under total 490 sets of conditions. The results are highly concentrated, as shown in Fig.5, and over 85% of them are in the range from 4.3 to 6.2, with the average of 5.34. The fact that $\zeta_{ac,p}$ is kept essentially constant suggests that Eq.(10) can describe the DP behaviour resulted from acceleration and collision of particles well. It should be noted that, as mentioned in Section 2.1.2, the variable u_{po} depends on L_{ac}, ρ_p/ρ_a and d_p for a certain u_a, as defined by Eqs.(4) and (5). Thus Eq.(10) includes actually all the factors affecting $-\Delta p_{ac,p}$. This may account for the phenomena that no difference was found between the values for $\zeta_{ac,p}$ obtained with millets and rape seeds, respectively. Therefore the following equation is recommended.

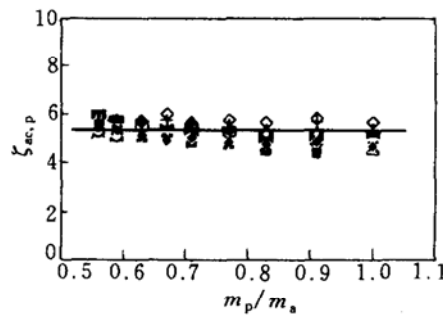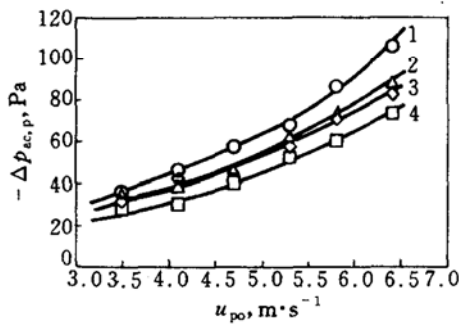$$-\Delta p_{ac,p} = 2.67 \rho_a \left(\frac{m_p}{m_a} \right) u_{po}^2 \qquad (20)$$

Figure 4 Effects of u_{po} and m_p/m_a on $-\Delta p_{ac,p}$ ($S/d = 4.0$)

curve	1	2	3	4
particles	rape seeds	millets	rape seeds	millets
m_p/m_a	0.769	0.769	0.588	0.588

Figure 5 Some of measured values for $\zeta_{ac,p}$
$(u_{po} = 3.51 - 6.42 \text{m} \cdot \text{s}^{-1})$

—— average value of totally 490 data;
◇□△ ×∗○ millets, $S/d = 5.0$;
+ ■◆ rape seeds, $S/d = 4.0$

4.4 Resistance caused by design of the ISC

As described in Section 3, $-\Delta p_{BC}$ or $-\Delta p_{B'C}$, the partial DP being measured directly, is the sun of $-\Delta p_{im}$ and $-\Delta p_{ds}$, but not any of the two, because both they are too small($<$ or ≈ 10Pa) to measure exactly, in addition to the fact that fluctuation of pressure occurs very often round the impingement zone. In the ISC tested here, the expression for $-\Delta p_{ds}$, Eq.(16), can be specified as

$$-\Delta p_{ds} = \frac{1}{2}\left(\frac{0.02116}{0.05}\right)^4 \rho_a u_a^2 = 0.016 \rho_a u_a^2 \tag{21}$$

Thus, $-\Delta p_{im}$ can be obtained for each run by

$$-\Delta p_{im} = [(-\Delta p_{BC}) + (-\Delta p_{B'C})]/2 - (-\Delta p_{ds}) \tag{22}$$

Table 3 gives two sets of typical data so obtained for $-\Delta p_{im}$ as instances. It follows that no influence of mass flow rate ratio, m_p/m_a, on $-\Delta p_{im}$ is found and the values calculated by Eq.(12) for the equivalent local resistance coefficient, ζ_{im}, are essentially constant, suggesting that $-\Delta p_{im}$ is independent of the existence of particles in suspension and Eq.(12) parallels the behaviour of DP resulted from impingement well. The value for ζ_{im} averaged over total 490 sets of data is 0.096. Therefore the expression below can be used

$$-\Delta p_{im} = 0.048 \rho_a u_a^2 \tag{23}$$

4.4 Model for total pressure drop over ISC

From the results described above the empirical model below is suggested

$$\begin{aligned}
-\Delta p_T &= \lambda_a \frac{L_{ac}}{d} \frac{\rho_a u_a^2}{2} + 2.67 \rho_a \left(\frac{m_p}{m_a}\right) u_{po}^2 + 0.048 \rho_a u_a^2 + \frac{1}{2} \zeta_{ds} \rho_a u_a^2 \\
&= \left(0.048 + \frac{\lambda_a}{2} \frac{L_{ac}}{d} + 0.5\zeta_{ds}\right) \rho_a u_a^2 + 2.67 \rho_a \left(\frac{m_p}{m_a}\right) u_{po}^2
\end{aligned} \tag{24}$$

for the total pressure drop across an ISC with two horizontal coaxial jets in the range of $S/d \geqslant 4$, where u_{po} is a function of u_a for certain values of L_{ac} and d and certain material system, and can be determined by integrating Eq.(5) from 0 to L_{ac}; λ_a depends mainly on roughness of the tubing used as the accelerating pipes, and is 0.0214 for the ISC used in this study as mentioned above; while ζ_{ds} depends on design of the ISC used. Calculations show that Eq.(24) fits the measured data well, as shown in Fig.6.

Table 3 Typical data indirectly measured for $-\Delta p_{im}$ and ζ_{im}

u_a, m·s^{-1}	$S/d=6.0$		$S/d=6.7$	
	$-\Delta p_{im}$,Pa	ζ_{im}	$-\Delta p_{im}$,Pa	ζ_{im}
9.48	4.90	0.091	4.30	0.079
11.06	6.84	0.093	6.81	0.092
12.64	7.47	0.081	7.48	0.081
14.22	10.76	0.088	11.09	0.091
15.80	13.38	0.089	12.85	0.085
17.36	15.95	0.088	15.12	0.083
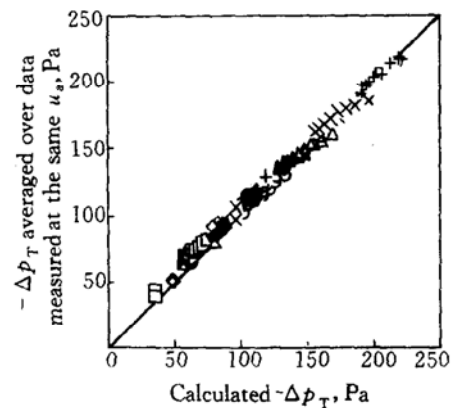
Figure 6 Comparison between calculated and measured overall pressure drops
u_a, m·s^{-1}: □ 9.48; ◇ 11.06; ○12.64; △ 14.22; × 15.60; + 17.36

It is clear from Eq.(24) that air velocity in the accelerating pipes, u_a, plays a very important role affecting the resistance of an ISC. Therefore, it is essential to choose a proper value for u_a. Too small u_a leads to poor effective impingement, on one hand, whereas too high u_a would bring about large power consumption, on the other.

4.5 A brief evaluation for power consumption of ISC

A comparison between ISC and other processing devices would be of interest. Although doing this is not easy because of the lack of operating data, it is still worth trying. The device similar to ISC in using pneumatic transport is the so-called flesh dryer. Table 4 gives a comparison between the two kinds of devices according to theoretical calculations, with taking particles of $d_p \approx 0.001$ m and $\rho_p \approx 1500$ kg · m^{-3} as the superficial material being processed, in which all the parameters for ISC are set to be unity for the basis. It follows from Table 4 that an ISC usually exhibits much higher efficiency and thus needs smaller processing space, while does not require large power for operation in comparison with a flesh dryer.

Table 4 A relative comparison between ISC and flesh dryer with the same capacity

Device	Operating air velocity	Maximum relative velocity	Mean transfer coefficient	Total length of pneumatic pipe	Effective processing time	Overall pressure drop	Specific power requirement
ISC	1	$1(\rightarrow 2u_a)$	1	1	1	1	1
flesh dryer	0.3—0.5	$0.1-0.2(=u_t<u_a)$	0.1—0.2	5—10	3—5	1—3	1—3

5 CONCLUSIONS

The resistance of an impinging stream contactor with two horizontal jets is studied both theoretically and experimentally in terms of overall pressure drop and its constituents. The conclusions that can be drawn from the results are

(1)The magnitude of the total pressure drop across the ISC studied is in an acceptable range;

(2)A large proportion of the power ($\geqslant 80\%$) used for operation of the ISC is being consumed in the acceleration of particles;

(3)The pressure drop resulted from impingement between suspension streams is independent of the presence of particles;

(4)The proposed models for the total pressure drop and its constituents that resulted from acceleration and collision of particles and that caused by impingement between streams, Eqs. (24), (20), and (23), respectively, parallel the related behaviours well.

NOMENCLATURE

a proportional coefficient
C_f drag force coefficient
d diameter, specially inside diameter of accelerating pipe, m
L,l length and length variable, m

m	mass flow rate, $kg \cdot s^{-1}$
p	pressure, Pa
$-\Delta p$	pressure drop, Pa
Re	Reynolds number
S	impinging distance, m
t	time, s
u	velocity, $m \cdot s^{-1}$
ε	roughness, mm
λ	friction coefficient
μ	viscosity, $Pa \cdot s$
ρ	density, $kg \cdot m^{-3}$
ζ	local resistance coefficient

Subscripts

a	air
ac	acceleration
b	bulk
c	resulted from collision
ds	design factor resulting in resistance
im	impingement
o	output or at outlet port
p	particles
T	total or overall
t	terminal

REFERENCES

1   Wu, G.A. and Wu, Y., Proc, 8th Chem. Engng. Conf., CHINA, Tianjin University, Tianjin (1996).

2   Tamir, A., Impinging Stream Reactors – Fundamentals and Applications, Eelsevier, Amsterdam (1995).

3   Mujumdar, A. S., *Drying Technology*, 9(2), 325 (1991).

4   Bar, T. and Tamir, A., *The Canadian J. Chem. Engng.*, **68**, 541 (1990).

5   Luzzatto, K., Tamir, A. and Elperin, I., *AIChE J.*, **30**, 600 (1984).

6   Tamir, A., Luzzatto, K., Sartana, D. and Salomon, S. A., *AIChE J.*, **31**, 1744 (1985).

7   Tamir, A. and Shalmon, B., *Indus. & Engng. Chemistry Research*, **27**, 2238 (1988).

8   Perry, R. H. and Green, D., Chemical Engineers' Handbook, 6th ed., McGraw-Hill, New York (1984).

9   Beijing Institute of Iron and Steel Technology, Pneumatic Transport Equipment (in Chinese), The Peoples Traffic Press, Beijing (1974).

10   Elperin, I. T., Transport Processes in Opposing Jets (in Russ), Nauka I Tekhnica, Minsk (1972).